

Communication to the Editor

Effective Interaction between Star Polymers

A. Jusufi, M. Watzlawek, and H. Lwen

Macromolecules, **1999**, 32 (13), 4470-4473 • DOI: 10.1021/ma981844u • Publication Date (Web): 05 June 1999

Downloaded from <http://pubs.acs.org> on February 12, 2009

More About This Article

Additional resources and features associated with this article are available within the HTML version:

- Supporting Information
- Links to the 8 articles that cite this article, as of the time of this article download
- Access to high resolution figures
- Links to articles and content related to this article
- Copyright permission to reproduce figures and/or text from this article

[View the Full Text HTML](#)



ACS Publications
High quality. High impact.

Effective Interaction between Star Polymers

A. Jusufi, M. Watzlawek, and H. Löwen*[†]

Institut für Theoretische Physik II,
Heinrich-Heine-Universität Düsseldorf,
Universitätsstrasse 1, D-40225 Düsseldorf, Germany

Received November 30, 1998

Revised Manuscript Received March 22, 1999

Star polymers are hybrids between polymerlike entities and colloidal particles, establishing an important link between these different systems; for recent reviews see refs 1 and 2. The interpenetrability of two stars is governed by the number of arms (or functionality), f , i.e., the number of linear polymer chains attached to a central microscopic core. For $f = 1, 2$ one recovers a system composed only of linear chains while in the limit $f \rightarrow \infty$ one gets sterically stabilized spherical colloidal particles which behave like effective hard spheres.^{3,4} Recent research^{5–8} has mainly focussed on polymer conformations of a *single* star. The only relevant length scale of a single star is embodied in the spatial extension of the monomers around the core as given by the so-called corona diameter σ .

In order to predict macroscopic properties of a *concentrated* solution of *many* stars, one has, however, to proceed one step further: In any statistical theory, the effective interaction between the stars is a necessary input. This interaction, in general, comprises many-body terms. For concentrations which are not too high, i.e., smaller than or comparable to the overlap concentration $\rho^* \equiv 1/\sigma^3$, triplet and higher-order terms are small and the system is dominated by effective pairwise interactions. Recently, on the basis of scaling theory,⁹ an explicit analytical expression for the effective pair potential $V(r)$ was proposed in ref 10. This potential combines a logarithmic form of the interaction potential for core–core separations r smaller than σ with an exponentially decaying interaction of Yukawa-form for distances r larger than σ :

$$V(r) = \frac{5}{18} k_B T f^{3/2} \begin{cases} -\ln\left(\frac{r}{\sigma}\right) + \frac{1}{1 + \sqrt{f/2}}; & r \leq \sigma \\ \frac{1}{1 + \sqrt{f/2}} \left(\frac{\sigma}{r}\right) \exp\left(-\frac{\sqrt{f}}{2\sigma}(r - \sigma)\right); & r > \sigma \end{cases} \quad (1)$$

Note that the potential strength simply scales with the thermal energy $k_B T$ since the repulsion between the stars is of purely entropic origin having a good solvent in mind. Both the potential in eq 1 and its associated force $F(r) = -dV(r)/dr$ are continuous at $r = \sigma$, but $F(r)$ has an artificial cusp at $r = \sigma$. The prefactor of the logarithm is fixed by scaling theory⁹ while the exponential decay length $2\sigma/\sqrt{f}$ is the diameter of the outermost blob within the Daoud–Cotton model for one star polymer.⁵

For an arm number of $f = 18$, this potential was tested against neutron scattering data, and reasonable agree-

ment was found.¹⁰ Further experimental support comes from shear moduli measurements in the crystalline phase of many-arm micelles.¹¹ Still, the scaling theory assumptions are strictly speaking only justified for core–core distances r much smaller than σ , and the exponential decay length of the outermost blob size is an heuristic assumption. Hence the validity of the potential for arbitrary arm numbers can be questioned. In this paper, we test the pair potential against a microscopic model, resolving the monomers of the chains, by extensive molecular dynamics computer simulations. To be specific, we use a simulation model for star polymers developed by Grest et al.,⁶ which was applied in previous studies for single stars, and generalize it to a situation with two stars, which is the minimal setup to extract information about the effective interaction between two stars. The distance-resolved interaction force $F(r)$ is calculated for arm numbers f ranging from $f = 5$ to $f = 50$. Each arm contains N monomers where N is varied from 50 to 200. As a result, we confirm the phenomenological interaction potential in eq 1; our simulation results are in perfect *quantitative* agreement with the theoretical prediction. This important result enables a mapping of a star polymer solution onto a classical one-component fluid¹² interacting via the effective ultrasoft pair potential of eq 1, provided the star concentration does not exceed ρ^* . This picture was anticipated in recent work, calculating the anomalous structure factor of star polymer solutions¹³ and the unusual phase diagram including re-entrant melting^{9,14} and anisotropic crystal structures.¹⁴ So, our present work provides a theoretical justification of all these previous studies.

Let us first describe the simulation model:⁶ Each polymer arm consists of N effective monomers or “beads” interacting via a purely repulsive Lennard–Jones-like potential $V_0(r)$, where r is the separation of the beads. $V_0(r)$ is obtained from the usual Lennard–Jones potential $V_{LJ}(r)$ by cutting $V_{LJ}(r)$ at the position of the potential minimum $r_m = 2^{1/6}\sigma_{LJ}$ and by shifting it by the constant value $V_{LJ}(r_m)$ in order to obtain $V_0(r_m) = 0$:

$$V_0(r) = \begin{cases} 4\epsilon \left[\left(\frac{\sigma_{LJ}}{r}\right)^{12} - \left(\frac{\sigma_{LJ}}{r}\right)^6 + \frac{1}{4} \right]; & r \leq 2^{1/6}\sigma_{LJ} \\ 0; & r > 2^{1/6}\sigma_{LJ} \end{cases} \quad (2)$$

Here, ϵ sets the energy scale and σ_{LJ} the length scale of the beads. The pure repulsion implies that we are dealing with a good solvent. For neighbouring beads along the chains, the attractive FENE-potential⁶ $V_{ch}(r)$ is added to the interaction

$$V_{ch} = \begin{cases} -15\epsilon \left(\frac{R_0}{\sigma_{LJ}}\right)^2 \ln \left[1 - \left(\frac{r}{R_0}\right)^2 \right]; & r \leq R_0 \\ \infty; & r > R_0 \end{cases} \quad (3)$$

This interaction diverges at $r = R_0$, which determines the maximum relative displacement of two neighbouring beads. Henceforth, we fix R_0 to be $1.5\sigma_{LJ}$. Then the total potential $V_0(r) + V_{ch}(r)$ between neighbouring monomers has a minimum at $r \approx 0.97\sigma_{LJ}$. Furthermore, the central core particles of the two stars have a finite hard core radius R_c , and all monomers are interacting with the

[†] Also at: IFF, Forschungszentrum Jülich, D-52425 Jülich, Germany.

core particles via a modified repulsive interaction potential $V_0^e(r)$. The introduction of a small hard core of the central particles of the stars is necessary to accommodate the large number of arms at small distances from the core.⁶ Thus we take explicitly for the potential

$$V_0^e(r) = \begin{cases} \infty; & r \leq R_c \\ V_0(r - R_c); & r > R_c \end{cases} \quad (4)$$

In addition, the innermost monomers of each arm are interacting with their core via an attractive potential which is given by

$$V_{ch}^e(r) = \begin{cases} \infty; & r \leq R_c \\ V_{ch}(r - R_c); & r > R_c \end{cases} \quad (5)$$

We note that exactly this simulation model was already used by Grest et al. in their simulations of single star polymers.⁶ In our simulations, the centers of the two stars are fixed at positions \vec{R}_1 and \vec{R}_2 with a given distance $r = |\vec{R}_1 - \vec{R}_2|$. The total number of mobile monomers is $2fN$, which limits our studies to small f and small N . In all simulations, the system is held at fixed temperature $T = 1.2\epsilon/k_B$. Under these circumstances, the effective force \vec{F}_i acting on the i th star center is given as a canonical average

$$\vec{F}_i = \langle -\nabla_{\vec{R}_i} \left(\sum_{k=1}^{2fN} V_0^e(|\vec{r}_k - \vec{R}_i|) + \sum_{j=1}^f V_{ch}^e(|\vec{r}_j - \vec{R}_i|) \right) \rangle \quad (6)$$

where in the first sum the repulsive interactions of the core with *all* $2fN$ monomers in the system are considered, whereas the second sum only accounts for the attractive interactions with the f innermost monomers of the chains attached to the i th center. Obviously, due to symmetry, $\vec{F}_1 = -\vec{F}_2$. We use standard molecular dynamics simulations¹⁵ to equilibrate the monomers and perform the statistical average $\langle \dots \rangle$ over the monomers for the forces on the star centers. The timestep is typically $\delta t = 0.002\tau$ (with $\tau = \sqrt{m\sigma_{LJ}^2/\epsilon}$ being the associated time unit and m the monomer mass) and typically 120 000 steps are used for equilibration and up to $t_{\max}/\delta t = 500\,000$ steps were simulated to gather statistics. It was carefully checked by monitoring the internal energy that the system had equilibrated. A typical snapshot of two stars after equilibration is shown in Figure 1. As can be seen, the monomers of one star do not penetrate much into the central region of the other star.

In order to check the code, we performed simulations of single stars changing the arm numbers between $f = 5$ and $f = 50$ and the monomer numbers from $N = 50$ to $N = 200$. The corresponding results for the radius of gyration $R_G^2 = 1/fN \langle \sum_{i=1}^N (\vec{r}_i - \vec{r}_{CM})^2 \rangle$ (where \vec{r}_{CM} is the center of mass of the whole star) and the density profile of the monomers are in very good agreement with the results given in ref 6 and are well described by the scaling theory of Daoud and Cotton.⁵ For a detailed list of the simulation parameters and the results for R_G , obtained from these single star simulations, see Table 1.

It should be noted that the effective forces on the star centers are the gradient of the *effective* star-star potential. This effective potential, however, differs in general from the monomer averaged potential energy of the star centers.¹⁶ We therefore had to calculate the averaged

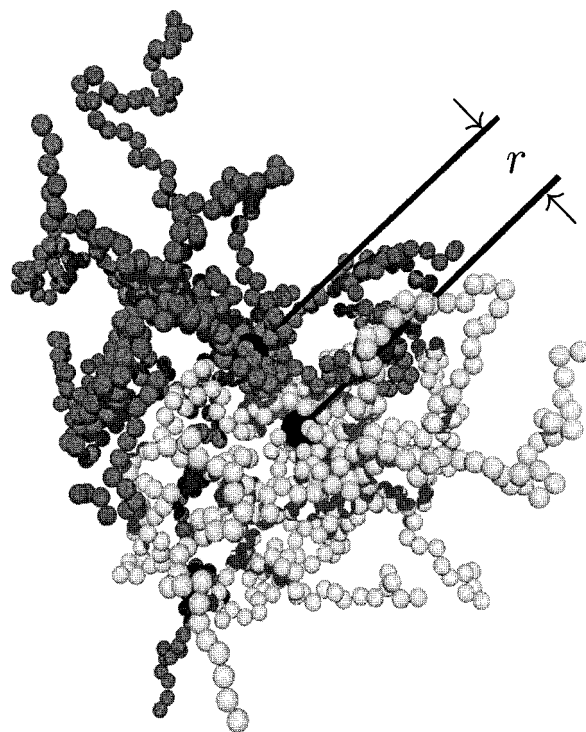


Figure 1. Typical configuration for two stars with $f = 10$ and $N = 50$. The distance between the central core particles, which are shown as big black spheres, is $r = 5.2\sigma_{LJ}$. The gray and light gray monomers belong to the first and second star respectively.

Table 1. List of the Simulation Parameters and the Corresponding Results for R_G and $\lambda = \sigma/2R_G$

f	N	$\delta t/\tau$	$t_{\max}/\delta t$	R_G/σ_{LJ}	$(R_G/\sigma_{LJ}) + 1/2$	R_G/σ_{LJ}	λ
5	100	0.004	500 000	13.53	0.65	1.39	0.61
10	50	0.003	400 000	10.37	1.1	1.21	0.66
10	100	0.003	400 000	16.18	1.1	0.89	0.64
10	150	0.003	400 000	19.71	1.1	1.31	0.60
10	200	0.003	400 000	24.52	1.1	1.42	0.67
18	50	0.002	350 000	11.19	1.25	1.38	0.68
18	100	0.002	350 000	17.10	1.25	1.64	0.65
30	50	0.002	350 000	12.22	1.6	1.89	0.66
50	50	0.002	350 000	13.35	1.8	2.40	0.69

forces \vec{F}_i ($i = 1, 2$) from our two star simulations to compare with the theoretical force as calculated from eq 1. In doing this, two difficulties arise: (i) The corona diameter σ , which is the relevant length scale in the potential of eq 1, is not known *a priori*. (ii) In contrast to the theory, there is a finite core size R_c in our simulation model.

As regards the first difficulty, σ is usually defined as the typical maximum range where a scaling behaviour of the monomer density around a single star center holds.^{5,9} A statistical definition of σ , however, is missing. On the other hand, the radius of gyration R_G has a clear definition as a canonical average, which can be calculated directly in simulations. We therefore use R_G , which was calculated in the single star simulations, as basic length scale for our simulation data and fit these data for $F = |\vec{F}_i|$ ($i = 1, 2$) to the theoretical prediction for $F(r)$ using the least-square method and treating σ as the single fit parameter. Afterward, we check how the optimal value for σ scales with R_G as obtained from the single star simulations. The procedure is consistent if the ratio $\lambda = \sigma/2R_G$ is independent of f . The second difficulty is resolved as follows: A logarithmic potential for $r < \sigma$ implies that the data should fall on a straight

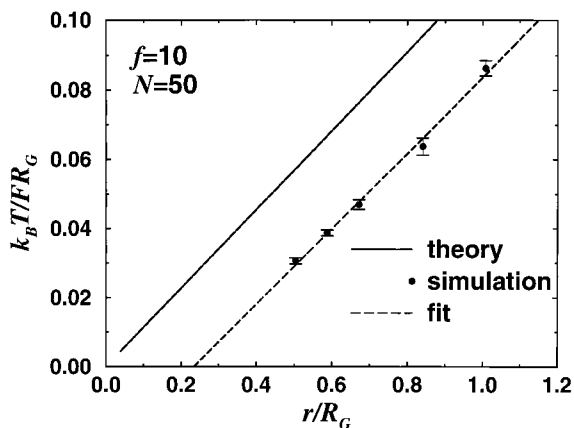


Figure 2. Reduced inverse force $k_B T / (FR_G)$ between the centers of two star polymers (for $f=10$ and $N=50$) vs reduced distance r/R_G . The error bars were obtained by averaging over the results of eight independent simulations.

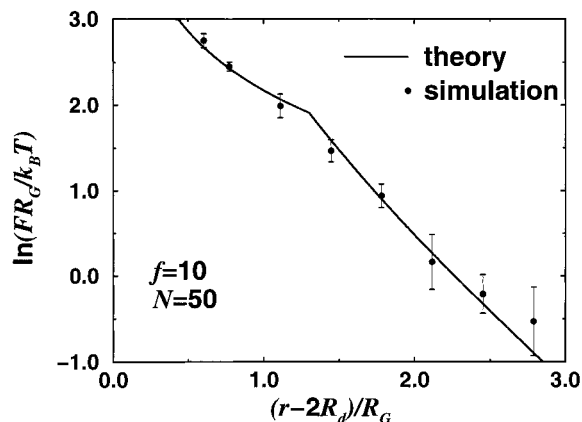


Figure 4. Logarithm of the reduced force $\ln(FR_G / (k_B T))$ vs reduced distance $(r - 2R_d) / R_G$ for $f=10$ and $N=50$. The error bars were obtained by averaging over the results of eight independent simulations.

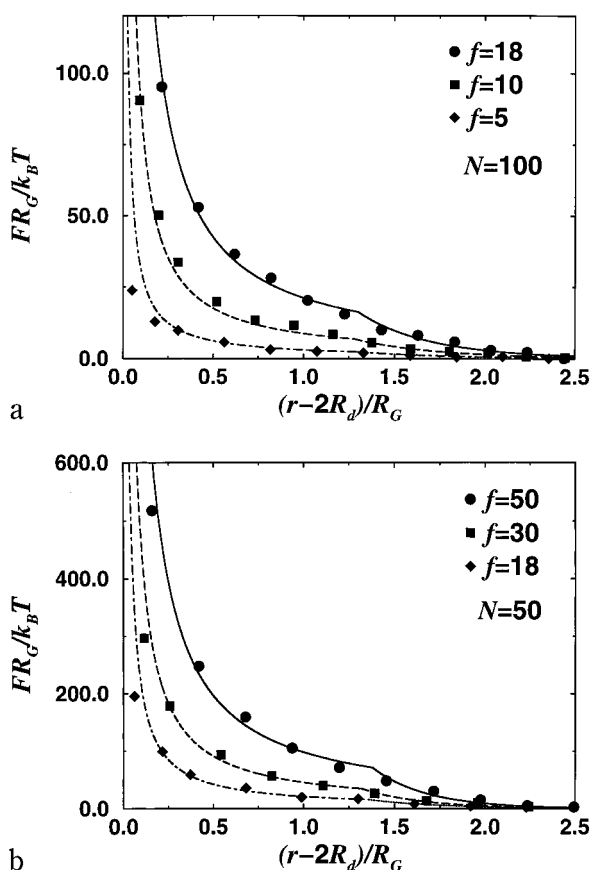


Figure 3. Simulation results (symbols) and theoretical results (lines) for the reduced effective force $FR_G / (k_B T)$ vs reduced distance $(r - 2R_d) / R_G$: (a) for $f=5, 10,$ and 18 and $N=100$; (b) for $f=18,$ and $30, 50$ and $N=50$.

line crossing the origin if one plots the *inverse force*, $1/F$, vs r inside the corona diameter. A typical plot is given in Figure 2. In fact, the data fall on a straight line. Extrapolating the data, however, one does not hit the origin. The divergence of the force occurs already at a finite distance $2R_d \approx 2R_c + \sigma_{LJ}$, which clearly has to be attributed to the presence of the finite core in the simulations. We note that both R_c and R_d have microscopic length scales and are of the same order of magnitude (see Table 1), thus being irrelevant for the macroscopic length σ in the scaling regime. We therefore normalize our distances by subtracting $2R_d$, thus match-

ing the divergence of the force properly. We emphasize that the slope of the straight line is in very good agreement with the theoretical prediction; see again Figure 2. This implies that the theoretical prefactor $^{5/18} f^{3/2} k_B T$ in eq 1 is confirmed by the computer simulations. In Figure 3, we show the effective force vs distance for five different arm numbers f and two monomer numbers N . The agreement with the theory is convincing for all f and N . The consistency of our fitting procedure of the corona diameter σ is documented in Table 1, where the ratio $\lambda = \sigma / 2R_G$ is given for different f and N . We find $\lambda \approx 0.65$ independent of f . This value also coincides with the value used in ref 10 to fit experimental data for $f=18$. We further note that λ is independent of N , consistent with scaling theory. Finally, we prove the exponential decay of the force for distances larger than σ by plotting the logarithm of the force vs distance in Figure 4 for one typical example. One clearly sees the crossover of the inner-core data to a straight line outside the core. The slope is consistent with the theoretical one as determined by the outermost blob size.

In conclusion, we have verified the ultrasoft pair interaction for star polymers by direct molecular simulations. It is straightforward to generalize the method to two stars confined in a periodically repeated cubic cell in order to estimate the shrinking of the corona diameter due to a finite star density. Also, similar to charged colloids,¹⁷ triplets of stars should be considered to investigate the importance of triplet interactions. Our future work lies along these directions.

Acknowledgment. We thank M. Schmidt and C. N. Likos for helpful remarks. M.W. thanks the Deutsche Forschungsgemeinschaft for support within SFB 237.

References and Notes

- (1) Grest, G. S.; Fetters, L. J.; Huang, J. S.; Richter, D. *Adv. Chem. Phys.* **1996**, *XCIV*, 67.
- (2) Gast, A. P. *Langmuir* **1996**, *12*, 4060.
- (3) Pusey, P. N. In *Liquids, Freezing and Glass Transition*; Hansen, J. P., Levesque, D. L., Zinn-Justin, J., Eds.; North Holland: Amsterdam, 1991.
- (4) Löwen, H. *Phys. Rep.* **1994**, *237*, 249.
- (5) Daoud, M.; Cotton, J. P. *J. Phys.* **1982**, *43*, 531.
- (6) Grest, G. S.; Kremer, K.; Witten, T. A. *Macromolecules* **1987**, *20*, 1376. Grest, G. S. *Macromolecules* **1994**, *27*, 3493.
- (7) Shida, K.; Ohno, K.; Kimura, M.; Kawazoe, Y.; Nakamura, Y. *Macromolecules* **1998**, *31*, 2343. Sikorski, A.; Romis-

- zowski, P. *J. Chem. Phys.* **1998**, *109*, 6169. Batoulis, J.; Kremer, K. *Macromolecules* **1989**, *22*, 4277. Freire, J. J.; Pla, J.; Rey, A.; Prats, R. *Macromolecules* **1986**, *19*, 452. Ishizu, K.; Ono, T.; Uchida, S. *Macromol. Chem. Phys.* **1997**, *198*, 3255. Forni, A.; Ganazzoli, F.; Vacatello, M. *Macromolecules* **1997**, *30*, 4737.
- (8) Willner, L.; Jucknischke, O.; Richter, D.; Roovers, J.; Zhou, L.-L.; Toporowski, P. M.; Fetters, L. J.; Huang, J. S.; Lin, M. Y.; Hadjichristidis, N. *Macromolecules* **1994**, *27*, 3821. Richter, D.; Jucknischke, O.; Willner, L.; Fetters, L. J.; Lin, M.; Huang, J. S.; Roovers, J.; Toporovski, C.; Zhou, L. L. *J. Phys. IV* **1993**, *3*, 3. Willner, L.; Jucknischke, O.; Richter, D.; Farago, B.; Fetters, L. J.; Huang, J. S. *Europhys. Lett.* **1992**, *19*, 297.
- (9) Witten, T. A.; Pincus, P. A. *Macromolecules* **1986**, *19*, 2509. Witten, T. A.; Pincus, P. A.; Cates, M. E. *Europhys. Lett.* **1986**, *2*, 137.
- (10) Likos, C. N.; Löwen, H.; Watzlawek, M.; Abbas, B.; Jucknischke, O.; Allgaier, J.; Richter, D. *Phys. Rev. Lett.* **1998**, *80*, 4450.
- (11) Buitenhuis, J.; Förster, S. *J. Chem. Phys.* **1997** *107*, 262.
- (12) See, e.g.: Hansen, J. P.; McDonald, I. R. *Theory of Simple Liquids*, 2nd ed.; Academic Press: London, 1986.
- (13) Watzlawek, M.; Löwen, H.; Likos, C. N. *J. Phys. Condensed Matter* **1998**, *10*, 8189.
- (14) Watzlawek, M.; Likos, C. N.; Löwen, H. *Phys. Rev. Lett.*, in press.
- (15) See, e.g.: Allen M. P.; Tildesley, D. J. *Computer Simulation of Liquids*; Clarendon Press: Oxford, England, 1989.
- (16) Löwen, H. *Prog. Colloid Polym. Sci.* **1998**, *110*, 12.
- (17) Löwen, H.; Allahyarov, E. *J. Phys. Condensed Matter* **1998**, *10*, 4147.

MA981844U